Third International Conference on CFD in the Minerals and Process Industries
CSIRO, Melbourne, Australia
10-12 December 2003

NUMERICAL SIMULATION OF TWO-DIMENSIONAL CERAMIC CANDLE FILTER FLOW

M. H. AL-HAJERI [1] and M. R. AL-AJMI [2]

[1] Faculty of Technological Studies, P.o.Box 34000, Roudha, Kuwait, (hajeri@paaet.edu.kw)
[2] A. Projects Department, MOD, Kuwait

ABSTRACT

This paper reports a computational study using CFD on a hot gas filter in cross flow arrangement. The filter generally operates with the dirty gases passing through the filter elements, the particulate material being deposited on the outside of the filter. However, in power co-generation plants, hot gas filtration is needed to allow the hot exhaust gases to be fed to a turbine without causing any physical damage to the blades.

The aim of this work is to increase understanding of the deposition process and the factors that affect the build up of the filter cake. A parametric investigation is undertaken with particular emphasis on the effects of the ratio of the approach cross flow velocity to filter face velocity on the deposition pattern as a function of the particle size (1 to 100 microns). Velocity fields and particle tracks are presented, in addition to the radius of convergence which is a parameter that characterizes the deposition process for each flow regime.

NOMENCLATURE

V_f- face velocity or filtration velocity.
V_i - upstream approach velocity or inlet velocity.
V_R - velocity ratio (v_i/v_f).
μ- viscosity.
ρ_p- density of particle.
cvcf- constant velocity cross flow
d_p- particle diameter.
d_f- filter diameter.
D_L- separation of last impinging trajectory
R_c - radius of convergence.
R_d - D_L/d_f Ratio
St- Stokes number.

INTRODUCTION

A ceramic candle filter element generally consists of a long slender hollow tube closed at one end. It is made of porous silicon carbide, with a grain size such that the hot gas can pass through and the particulate cannot. Stringer et al (1991) and Higashi (1992) and carried out an experimental investigations of ceramic candle filters. At Aachen university (EPRI (1992)vol 2), an array of six candle filter elements was mounted downstream of a combustor. Whilst an array of 130 candle filter elements were investigated at Grimethorpe (EPRI (1992)vol 1). The ceramic candle filters were tested at various operating conditions to investigate the back pulse cleaning and cycle time duration. Aroussi et al (1996) studied the flow around the single ceramic candle filter using the particle image velocimetry (PIV) experimental technique. Aroussi et al (1999) investigated using computational fluid dynamics technique the flow around ceramic candle filter with a porous boundary in cross-flow arrangement.

The filter element which is considered here has the configuration where the dirty gases are on the outside of the filter with cleaned gas passing to the inside of the candle. As the hot gases are filtered, the particulate material deposits on the outside of the filter element forming a filter cake. The cake is periodically removed by back-pulsing the filter. The ease and efficiency of cake removal is a fundamental design consideration and is clearly affected by the particle deposition distribution. The CFD work described in this paper, looks specifically at particle trajectories around filter element as a function of particle size and filter velocity. A computational method is used to conduct a parametric investigation taking into account all the factors that affect the filtration process in the configuration examined.

GEOMETRY

The Grimethorpe report (EPRI (1992)vol 1) investigated an array of 130 candle filter elements which are made by Schumacher and assembled in a radial arrangement. These filter elements have an inner diameter of 30 mm and 15 mm wall thickness. In this study, a single ceramic candle filter is considered and figure 1 shows the two-dimensional physical outline of the model. These dimensions are used in this investigation and figure 2 shows the dimensions of the full computational geometry which is used for the present CFD calculations.

The computational domain models are a two-dimensional horizontal slice of a single filter through an array of the candle filters, and only half of the geometry is modelled to save computational time and space. A body fitted co-ordinate grid of 160x80x1 (12800) computational cells is constructed in FLUENT's mesh generation program preBFC.

BOUNDARY CONDITIONS

This model has two inlets. The main inlet in the problem is referred to as inlet 1. This is an external boundary with a pre-defined inlet velocity (V_i) set for each case according to the face filtration velocity (V_f) and velocity ratios. Here, the inlet velocity is the approach velocity of the flow. Due to Fluent's inability to model porous outlets that are not attached to the physical boundaries of the problem, an

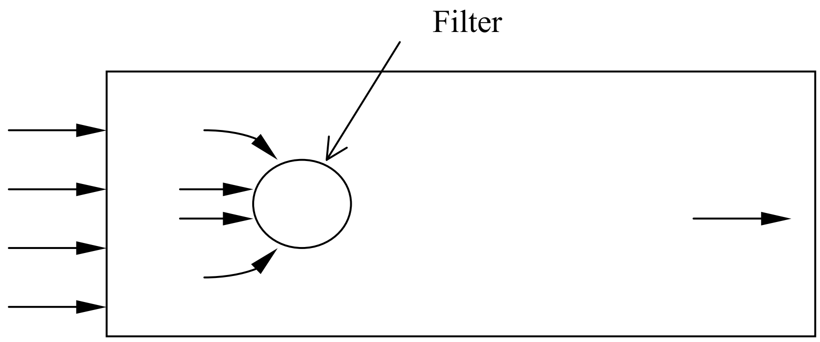

Figure 1. Single ceramic candle filter in cross flow.

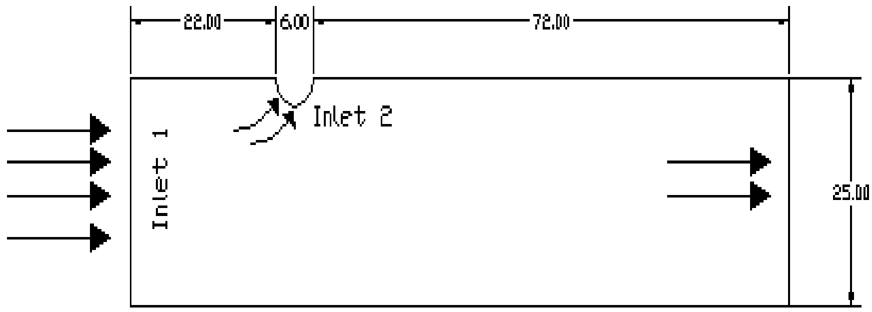

Figure 2. Computational geometry of single candle filter.(Dimensions in centimetre)

alternative method to define the outlet as a set inlet boundary at the face of the filter with appropriately defined constant velocity is employed. That is the simplest boundary condition to use and is appropriate because of high-pressure drop across the filter element relatively low gas velocities. This will also solve the problem of not being able to define more outlets than inlets.

The second inlet in the geometry is that at the face of the filter, and it is modeled as a half cylinder, and it is clearly shown in figure 2. Assuming a constant pressure drop across the filter element, a constant face velocity at the inlet 2 must prevail. However, constant u-velocity or v-velocity boundary condition cannot be achieved. Instead, polynomial curve fitted function boundary condition can successively apply and will give a constant face velocity (V_f) at any radii around the filter element.

A third degree polynomial curve fitted function is used in cross flow constant velocity cases (CVCF) to specify x and y velocity components of various locations, around the circumference of the filter. A variety of V_i values are obtained, by assuming various velocity ratios between velocities V_i and $V_{f\ and}$ using various face velocities. These values are then set as boundary conditions at inlet 1. In total four different face velocities where used along with six different face velocity ratios. This gives 24 different cases listed in table 1 and used for this study. The face velocities are found at Grimethorpe investigation (EPRI (1992)vol 1).

DISCUSSION OF THE RESULTS

The aim of this work is to carry out a parametric study for a ceramic candle filter in various arrangements. The flow around the filters may be categorized as cross flow, parallel flow or turning flow. The flow at the outside of the filter array is usually cross flow but in the middle becomes parallel flow while at the bottom of the array the flow is turning flow (EPRI (1992)vol 1). The face velocity into each filter is the same irrespective of the position in the array, as the pressure difference across each element is large compared to the dynamic pressure of the flow approaching and within the filter array.

Since the filters are quite long (50 cm) relative to their diameter (6 cm), this arrangement becomes very similar to that for flow around tube banks. However, an important difference here is the existence of a normal velocity component to the filter element due to the filtration effect. This is a point that will legitimize a two-dimensional treatment, where cross flow is concerned, is realistic. A further simplification to the problem is through the use of a symmetry line through the centreline of a single filter element as shown in figure 2.

Particle trajectories around a single filter were investigated for different size, face velocities and inlet velocities. Face velocities will vary and values of 2, 3, 4 and 5 cm/s which are found at Grimethorpe (EPRI (1992)vol 1), are used. Inlet velocities vary according to the velocity ratio $V_i/V_{f,}$ and V_i/V_f ratios range of 0.8, 1, 1.2, 1.6, 2 and 5 are used. Table 1 shows the 24 boundary condition which are used here in this study.

One of the main objectives of this work is to carry out a parametric study of the flow around the ceramic candle filter. A radius of convergence (R_c) as defined by Aroussi et al (1996) is a useful comparison criteria. It is defined as the distance from the filter centreline, at the main inlet, to the position of injection of the last particle which will impinge on the filter. Figure 3 shows the definition of the radius of convergence which is also called, the critical trajectory. The radius of convergence depends upon the inlet velocity, the particle size and the face velocity.

The calculation is a time consuming repetitive process where particles are injected at the inlet into the domain. This is repeated at various levels until a particle turning around the filter impinges on it at the point closest to the symmetry line behind the element. Spherically shaped particles having diameter of 1, 50 and 100 microns were injected with an assumed density of 1000 kg/m^3. Although, particle diameters between 1 to 50 microns are the main focus here, the results show that no change in the trajectory occurred for particles in the range 1 to 50 microns in this cross flow investigation. However, the radius of convergence varies if the particle has a diameter of 100 microns and larger.

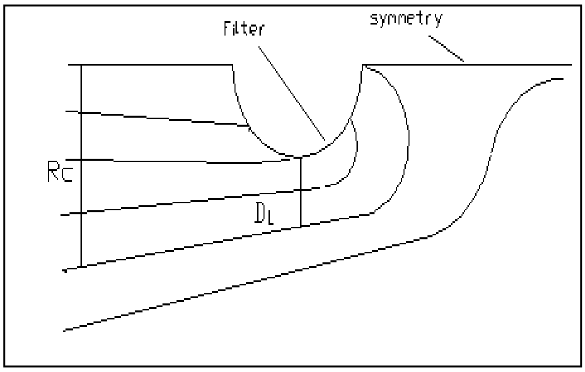

Figure 3. Definition of Radius of convergence (R_c) and separation distance of last impinging particle (D_L)

Figure 4 shows the relation between the radius of convergence (R_c) and the inverse of the inlet velocity ($1/V_i$) for the face velocity of 3 cm/s. The curves are straight lines and show R_c for the three particles size 1, 50 and 100 μm. These curves are almost identical but there is slight difference in the case of the high inlet velocity with a particle size of 100 μm (as stated earlier).

For the case with a face velocity of 5 cm/s, figure 5 shows the relationship between the radius of convergence and $1/V_i$. The graphs are straight lines and, as in the previous figure. At a high inlet velocity, the radius of convergence (R_c) for 100 μm particles diverges slightly in value. Overall, the three graph curves for 1, 50 and 100 μm have almost identical values for the radius of convergence. For three other velocities 2, 3 and 4 m/s, the curves have the same trends, however they have different values for the radius of convergence at different inlet velocities. So as the inlet velocity is increased, whilst the face velocity is kept constant, the radius of convergence is decreased. In conclusion, the V_i/V_f ratio is the main factor affecting the radius of convergence in the cross flow regime. The figure curves show that as the V_i/V_f ratio (V_R) decreases the radius of convergence increases.

A non dimensional analysis is a very useful comparison tool for the present problem. The Stokes number is appropriate for fluid-solid flow, and using Buckingham π-Theorem, Stokes number is defined by using the approach velocity as, (Crowe et al. (1985))

$$St = \frac{\tau_s}{\tau_f} \quad (1)$$

$$\tau_s = \frac{\rho_p d_o^{\ 2}}{18\mu} \quad (2)$$

$$\tau_f = \frac{d_f}{V} \quad (3)$$

where τ_s is the aerodynamic response time, τ_f is the time associated with the large-scale motion and μ is the kinematics viscosity of the fluid,:

$$\mathrm{St} = \frac{\rho_p d_p^2 V_i}{18\mu d_f} \quad (4)$$

Stokes number results are plotted here in two graphs with respect to non-dimensional radii of convergence. The radius of convergence (R_c) is divided by the filter diameter to obtain a non-dimensional form of R_c. Figure 6 shows the relationship between the radius of convergence to filter diameter with Stokes number for particle size 1 μm. The horizontal straight lines for each V_i/V_f ratio indicate that the radius of convergence does not change with Stokes number regardless of whether the face velocity or the inlet velocity is used for any particle having a diameter less than 100 microns. If particle diameter is increased and V_i/V_f ratio is kept constant, the radius of convergence decreases. Stokes number values range between 1 to 2.5 in the case size of 1 μm particles, and between 50 to 125 in case of 50 μm particles.

One of the important factors in designing ceramic candle filters or in the investigations of multiple filters is the spacing between any two-filter elements. Determining the spacing between the filters pre-requisites the knowledge of the radius of convergence and the V_i/V_f ratio which the filter will operate at. A new parameter (D_L) is introduced in this study which is the distance between the particle path of the furthest impinging trajectory and the surface of the filter nearest to it as shown in figure 3. This distance is measured perpendicular to the centerline in the present solution domain. This parameter is then used to define an important non-dimensional ratio R_d which is the ratio of the separation of the last impinging trajectory (D_L) to the filter diameter (D_L/d_f). D_L values are calculated based on particle trajectories of particle sizes of 1, 50 and 100 μm.

Figure 7 exhibits a plot of the D_L/d_f ratio against V_i/V_f. This is also shown in table 2 where D_L/d_f decreases with increase in V_i/V_f. However, as the inlet (approach) velocity increases whilst the face velocity is kept constant, the filter suction (and D_L consequently) will both decrease. Filter elements should, hence, be designed faraway from each other in the case of lower V_i/V_f ratios and close to each other in the case of higher V_i/V_f ratios. For rows of filters nearer to the inlet in an array, the filter elements should be spread out further to allow flow to pass between them to the next row. Also, trends of change in D_L/d_f ratio and D_L are identical for all V_i/V_f ratio cases regardless of the change in face and inlet velocity.

CONCLUSIONS

A computational investigation has been carried out into the flow around a single ceramic candle filter element in cross flow. The radius of convergence (R_c), the separation of the last impinging trajectory (D_L) and the velocity fields are used to explain the particles behavior and the filter cake distribution.

Three particle sizes of 1, 50 and 100 microns are tracked through the domain to determine Rc and D_L for several face velocities as well as several (inlet/ face) velocity ratios (V_i/V_F). It is found that the radius of convergence and the separation of the last impinging trajectory (D_L) decrease with the increase of V_i/V_f ratio and the reduction in R_c as the particle size increases. Also it is found that for any Stokes number and particle diameter smaller than 100 microns, Rc is constant. Filter cake distributions around the filter element surface are uniform for particle sizes below 50 microns. Thus, that can delay the cleaning periods and increase the filtration time. Results obtained here are essential for designing the cleaning mechanism.

REFERENCES

AROUSSI, A., AL-HAJERI, M., and PICKERING, S. J., 1999, " A parametric study of filtration through a ceramic candle filter in cross flow arrangement, " ASME 2nd International Symp. on Computational Technologist for Fluid, August, Boston, MA.

AROUSSI, A., SIMMONS, K. and PICKERING, S. J., 1996, "Removal of particulate material by ceramic candle filter, " IMechE S447/014/96, pp. 193-204.

EPRI1992, High-temperature gas filtration. Vol 2: Operating performance of a pilot-scale filter, EPRI Rept. GS-6489 vol. 2, October.

EPRI1992, Grimethorpe high-pressure/high temperature gas filter experimental program, Vol. 1. EPRI Rept. TR-100-499 vol. 1, September.

HIGASHI, O, "Development of high temperature, high-pressure filtration technology, " ASME paper 92-G7-370.

STRINGER, J., LEITCH, A.J. and CLARK, R.K., 1991, " THE EPRI hot gas filter pilot plant at Grimethorpe: what worked, what broke and where do we go now?, Fluidised Bed Combustion.

Case no.	V_f(cm/s)	V_i/ V_f	V_I(cm/s)
1	2	0.8	1.6
2	2	1	2
3	2	1.2	2.4
4	2	1.6	3.2
5	2	2	4
6	2	5	10
7	3	0.8	2.4
8	3	1	3
9	3	1.2	3.6
10	3	1.6	4.8
11	3	2	6
12	3	5	15
13	4	0.8	3.2
14	4	1	4
15	4	1.2	4.8
16	4	1.6	6.4
17	4	2	8
18	4	5	20
19	5	0.8	4
20	5	1	5
21	5	1.2	6
22	5	1.6	8
23	5	2	10
24	5	5	25

Table 1. Velocity boundary conditions and velocity ratios (V_f is face velocity, V_I is approach velocity

V_i/V_f	$R_d = (D_L/d_f)$	R_C (cm)	D_L (cm)
0.8	0.837	0.115	0.050
1	0.598	0.092	0.036
1.2	0.434	0.0745	0.026
1.6	0.325	0.0585	0.020
2	0.249	0.046	0.015
5	0.079	0.0184	0.005

Table 2. R_d (D_L/d_f ratio) and particle path distance V_i = 2 cm/s

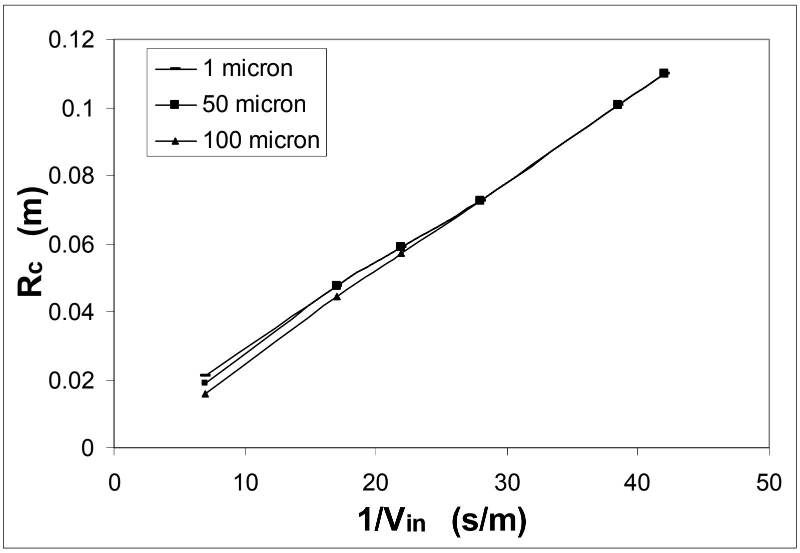

Figure 4. Variation of R_c with V_I for particle diameter of 1, 50 and 100 microns. (V_f=3 cm/s)

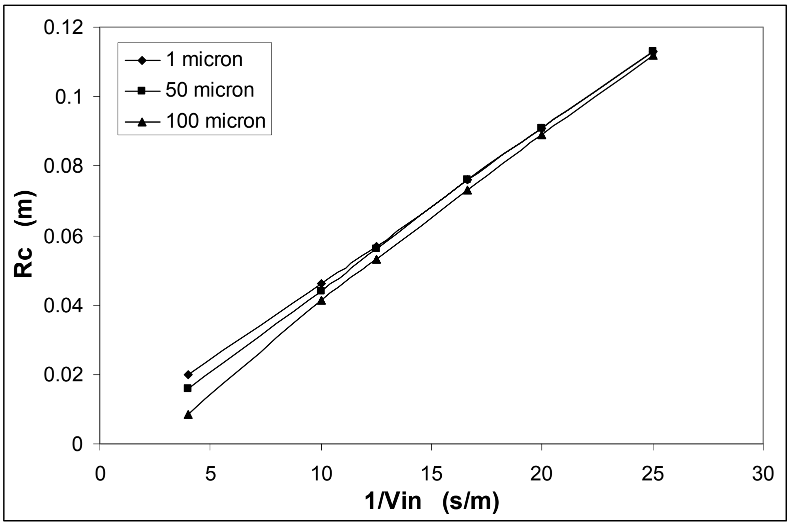

Figure 5. Variation of R_c with V_I for particle diameter of 1, 50 and 100 microns. (V_f=5 cm/s)

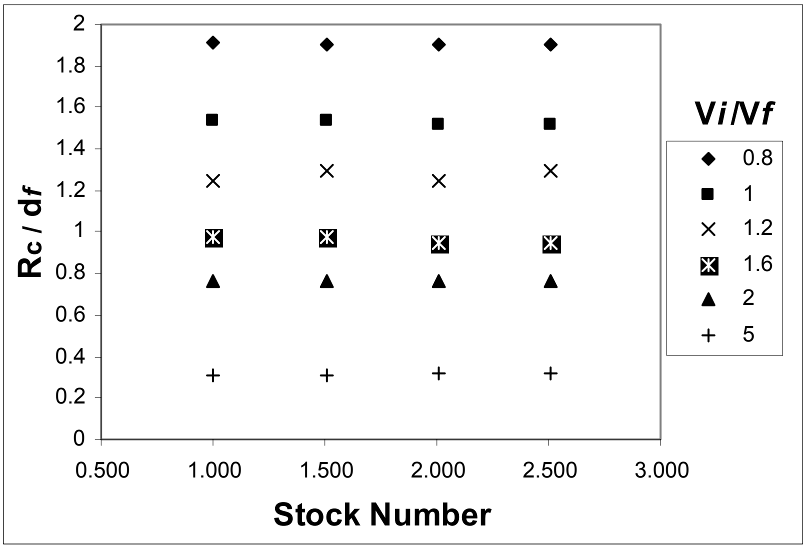

Figure 6. Variation of Stokes number with V_I for particle diameter of 1 microns. (V_f=5 cm/s)

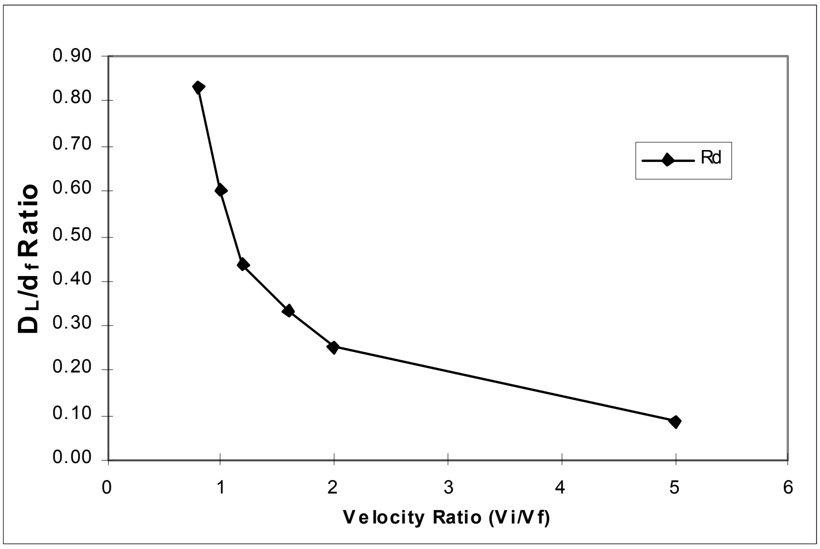

Figure 7. Variation of DL/d_f with $V_i/V_{f.}$ (V_f=2 cm/s)